Journal of Alloys and Compounds 520 (2012) 281–286

Contents lists available at SciVerse ScienceDirect

Journal of Alloys and Compounds

journal homepage: www.elsevier.com/locate/jallcom

Effect of Dy addition on mechanical and magnetic properties of Mn-rich Ni–Mn–Ga ferromagnetic shape memory alloys

L. Gao [a,*], G.F. Dong [b], Z.Y. Gao [c], W. Cai [c]

[a] College of Engineering Science and Technology, Shanghai Ocean University, Shanghai 201306, China
[b] Department of Physics, Dalian University, Dalian 116622, China
[c] School of Materials Science and Engineering, P.O. Box 405, Harbin Institute of Technology, Harbin, 150001, China

ARTICLE INFO

Article history:
Received 26 September 2011
Received in revised form 6 January 2012
Accepted 9 January 2012
Available online 15 January 2012

Keywords:
Ferromagnetic shape memory alloy
Rare earth element
Mechanical properties
Curie temperature

ABSTRACT

The effects of partial substitution of rare earth Dy for Ga on the mechanical and magnetic properties of Mn-rich $Ni_{50}Mn_{29}Ga_{21-x}Dy_x$ ($0 \le x \le 5$) ferromagnetic shape memory alloys were investigated in detail. The results show that an appropriate amount of Dy addition significantly improves the mechanical properties of Ni–Mn–Ga alloy. With an increase in Dy content, the compressive strength enhances rapidly at first and then becomes stable when the Dy content is more than 1 at.%. However, the compressive strain increases dramatically and reaches a maximum value with 1 at.% Dy addition. Further increase in Dy content makes the compressive strain of the alloys decrease gradually. The mechanism of the improved mechanical properties is also discussed. Moreover, Dy doping changes the fracture type from intergranular fracture of Ni–Mn–Ga alloy to transgranular cleavage fracture of Ni–Mn–Ga–Dy alloys. The Curie temperature remains almost unchanged at low Dy content and subsequently decreases.

1. Introduction

During the past few years, Ni–Mn–Ga alloys have been the subject of much interest due to their large magnetic field-induced strain (MFIS) and high response frequency [1–5]. For example, the response frequency of Ni–Mn–Ga alloy is up to be ~10 kHz. Moreover, a very large MFIS of 9.5% in 7 M martensite was achieved in $Ni_{48.8}Mn_{29.7}Ga_{21.5}$ single crystal [6]. All of these make Ni–Mn–Ga one of the strongest candidates for new magnetic actuators. However, Ni–Mn–Ga alloys exhibit extreme brittleness, low strength and poor processability, which greatly limit their applications. Recently, many attempts of alloying Ni–Mn–Ga alloys with rare earth elements have been carried out and some encouraging results have been achieved. It was reported that by adding rare earths Y, Tb, Gd or Nd to polycrystalline Ni–Mn–Ga alloy, significant improvements in the compressive strength and ductility were obtained [7–10]. In addition, the bending strength of Ni–Mn–Ga alloy was increased with the addition of Gd, Tb or Sm to some extent [11–13]. On the other hand, the addition of rare earths can affect the martensitic transformation temperatures. The decrease of martensitic transformation temperatures was observed in Ni–Mn–Ga–Sm alloy [13], while the martensitic transformation temperatures of Ni–Mn–Ga alloy containing Nd or Tb showed a small increase [10,12]. The current group discovered that the martensitic transformation temperatures of Ni–Mn–Ga alloys increased remarkably with the increase in Dy, Gd or Y content [14–16]. Meanwhile, a systematic investigation on martensitic transformation behavior and the precipitate phase in quaternary Heusler alloys of NiMnGaDy was also reported [17]. The results indicated that the Dy doping notably increased the martensitic transformation temperatures, i.e. the martensitic transformation start temperature rose from 326 to 512 K when the substitution of Dy for Ga was up to 5 at.%. The morphology and distribution of the Dy-rich precipitates in higher Dy-addition alloys were revealed, and the crystal structure and chemical formula were determined firstly. These findings are helpful in explaining the effects of Dy addition on various properties in Ni–Mn–Ga alloys. However, information on the effect of Dy addition on the mechanical property and fracture behavior of Mn-rich Ni–Mn–Ga alloys is still inadequate. In addition, the effect of adding Dy on magnetic properties needs to be clarified. Therefore, a further investigation on such compositional polycrystalline Ni–Mn–Ga–Dy alloys is urgent. The present paper focuses on the influence of Dy addition in Mn-rich $Ni_{50}Mn_{29}Ga_{21-x}Dy_x$ ($0 \le x \le 5$) alloys on the microstructure, mechanical and magnetic properties.

2. Experimental

The nominal composition of the alloys was $Ni_{50}Mn_{29}Ga_{21-x}Dy_x$ ($x = 0, 0.1, 0.5, 1, 2, 5$). These alloys were prepared with high purity element by melting four times in a non-consumed vacuum arc furnace under argon atmosphere, and then cast into rods 10 mm in diameter and 75 mm in length using a cylindrical copper mold set at the bottom of the furnace. The samples were annealed in vacuum quartz tubes at 800 °C

* Corresponding author. Tel.: +86 21 61900819; fax: +86 21 61900805.
E-mail addresses: lgao@shou.edu.cn, gaoli.99@163.com (L. Gao).

0925-8388/$ – see front matter © 2012 Elsevier B.V. All rights reserved.
doi:10.1016/j.jallcom.2012.01.048

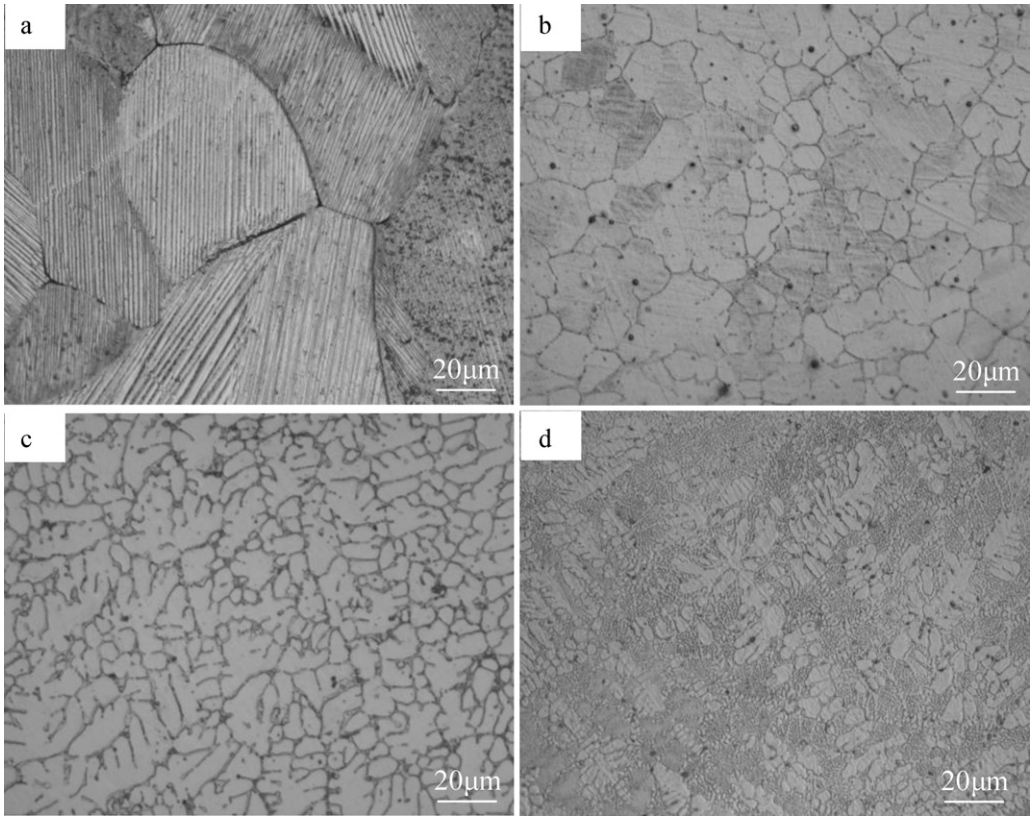

Fig. 1. Optical micrographs of $Ni_{50}Mn_{29}Ga_{21-x}Dy_x$ alloys. (a) $x = 0$; (b) $x = 1$; (c) $x = 2$ and (d) $x = 5$.

for 24 h, followed by water-quenching. Microstructures of the alloys were examined using an Olympus metallographic microscope and an MX2600FE scanning electron microscopy (SEM) equipped with an X-ray energy dispersive spectroscopy (EDS) analysis system. The compression tests were performed at room temperature on an Instron 5569 testing system at a crosshead displacement speed of 0.05 mm min^{-1}, and the size of the sample was 3 mm × 3 mm × 5 mm. Fractography was observed by MX2600FE SEM to study the dominant fracture behavior in this alloy system. The phase transformation temperatures were determined by Perkin-Elmer diamond differential scanning calorimetry (DSC), the rate of heating and cooling was 20 K/min. The Curie temperatures of the alloys were measured by AC susceptibility.

3. Results and discussions

3.1. Microstructure of $Ni_{50}Mn_{29}Ga_{21-x}Dy_x$ alloys

Fig. 1 shows the optical micrographs of $Ni_{50}Mn_{29}Ga_{21-x}Dy_x$ ($x = 0, 1, 2, 5$) alloys. It is shown that the ternary $Ni_{50}Mn_{29}Ga_{21}$ alloy in the present study displays coarse equiaxed grain. The average grain size is approximately 110 μm. The martensite variant along different direction inside the grains can be clearly seen and this indicates that the martensitic transformation start temperature of the alloy is above room temperature. Moreover, it is noticed that the addition of Dy results in the grain size reduce significantly. As seen in Fig. 1(b) and (c), the grain size tends to be smaller with higher Dy content. When the Dy content is 2 at.%, the grain size is reduced to 10 μm, approximately. At the same time, the second phase appears along the grain boundaries. A network-like distribution and local enrichment of the second phase are also observed in this alloy. As the content of Dy increases to 5 at.%, the amount of the second phase increases abundantly such that the matrix is segregated into many small islands. In this case, the grain boundaries are blurry, as shown in Fig. 1(d).

Fig. 2 shows the backscattered electron images of $Ni_{50}Mn_{29}Ga_{21-x}Dy_x$ alloys. Apparently, the Dy-containing alloys consist of the matrix and the white Dy-rich phase. When the content of Dy is 0.1 at.%, small amount of the Dy-rich phase sporadically disperses in the matrix. With the increase in Dy content, the volume fraction of the Dy-rich phases increases gradually. When the content of Dy increases from 0.5 at.% to 2 at.%, the Dy-rich phases gets distributed mainly along the grain boundaries. A eutectic structure composed of the matrix and the Dy-rich phases is observed in the alloy with Dy content up to 5 at.%. As shown in Fig. 2(e), the Dy-rich phases inside the grains have a lamellar morphology, whereas those along the grain boundaries are of irregular shape with larger size. According to the XRD and TEM measurements results [17], the Dy-rich precipitates can be indexed to $Dy(Ni,Mn)_4Ga$ phase with a hexagonal $CaCu_5$ type structure.

3.2. Mechanical properties of $Ni_{50}Mn_{29}Ga_{21-x}Dy_x$ alloys

In order to investigate the effect of rare earth Dy on the mechanical properties, compression tests were carried out at room temperature. All the samples were in the martensite at room temperature, and were compressed to fracture. Fig. 3 shows the compressive stress–strain curves of $Ni_{50}Mn_{29}Ga_{21-x}Dy_x$ alloys at room temperature. The effect of Dy content on the compressive strength and the compressive strain of $Ni_{50}Mn_{29}Ga_{21-x}Dy_x$ alloys are illustrated in Fig. 4. It is shown that both the compressive strength and strain have a strong dependence upon the Dy content. When the Dy content is less than 1 at.%, the compressive strength increases almost linearly as Dy addition increases, and the subsequent increase is more gradual when the Dy content is up to 2 at.%. As the Dy content further increases to 5 at.%, the compressive strength decreases slightly compared with that of $Ni_{50}Mn_{29}Ga_{19}Dy_2$ alloy. However, the compressive strain increases gradually and reaches a maximum value with 1 at.% Dy addition. Further increase of Dy content makes the compressive strain of the alloys decrease obviously. As mentioned above, the best comprehensive mechanical property is

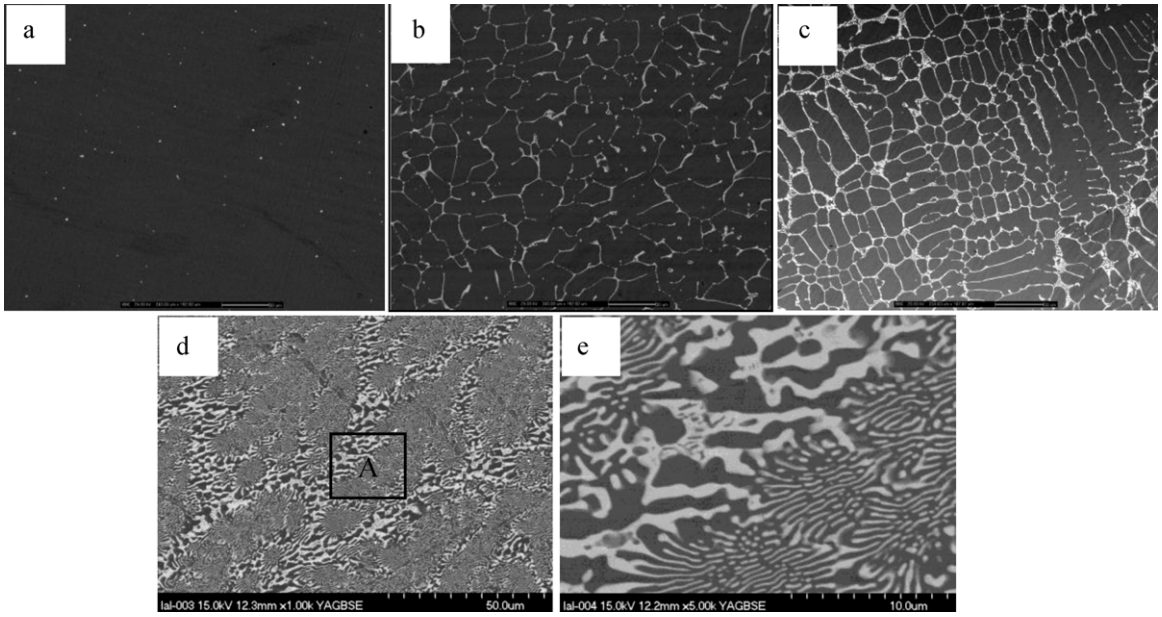

Fig. 2. Backscattered electron images of $Ni_{50}Mn_{29}Ga_{21-x}Dy_x$ alloys. (a) $x = 0.1$; (b) $x = 1$; (c) $x = 2$; (d) $x = 5$ and (e) the magnification of region A in (d).

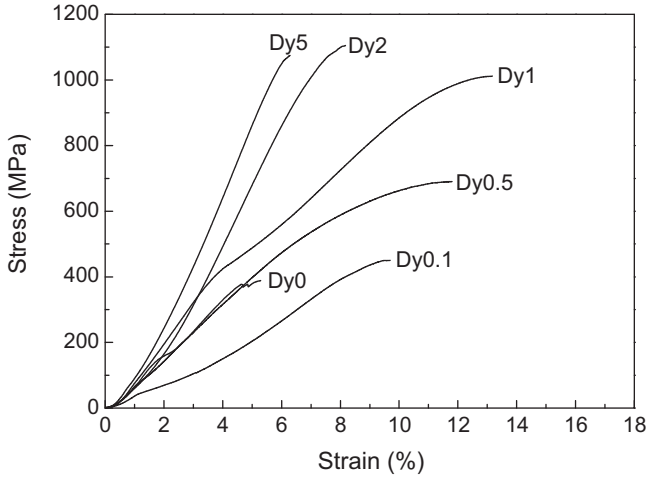

Fig. 3. The compressive stress–strain curves of $Ni_{50}Mn_{29}Ga_{21-x}Dy_x$ alloys at room temperature.

obtained in $Ni_{50}Mn_{29}Ga_{20}Dy_1$ alloy. This clearly suggests that the proper Dy addition significantly enhances the compressive strength and improves the ductility of the alloys.

The reason for the improvement of mechanical properties in $Ni_{50}Mn_{29}Ga_{21-x}Dy_x$ ($x = 0$–5) alloys may be explained as follows. When the content of Dy is 0.1 at.%, the alloy still exhibits coarse grains. The enhancement of the compressive strength may be closely related to the purification of rare earth Dy. Rare earth easily reacts with the impurity elements, such as O and S, restraining the segregation of the impurities at the grain boundaries. The grain boundaries are consequently strengthened, which leads to an increase in the compressive strength. When the content of Dy increases from 0.5 at.% to 1 at.%, the microstructure reveals that the average grain size decreases from 95 to 30 μm. Therefore, the refinement of the grains may account for the improvement of compressive strength and strain. At the same time, the size and distribution of $Dy(Ni,Mn)_4Ga$ phase have a great effect on the compressive properties of $Ni_{50}Mn_{29}Ga_{21-x}Dy_x$ alloys. With the increase in Dy content, the $Dy(Ni,Mn)_4Ga$ phase becomes larger and tends to distribute along the grain boundaries. The discontinuous distribution of the $Dy(Ni,Mn)_4Ga$ phase at the grains boundaries

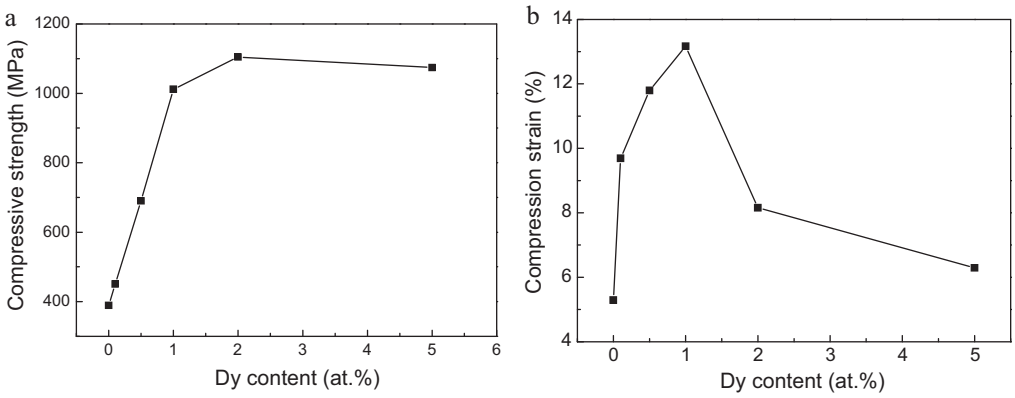

Fig. 4. Effect of Dy content on the compressive strength (a) and the compressive strain (b) of $Ni_{50}Mn_{29}Ga_{21-x}Dy_x$ alloys.

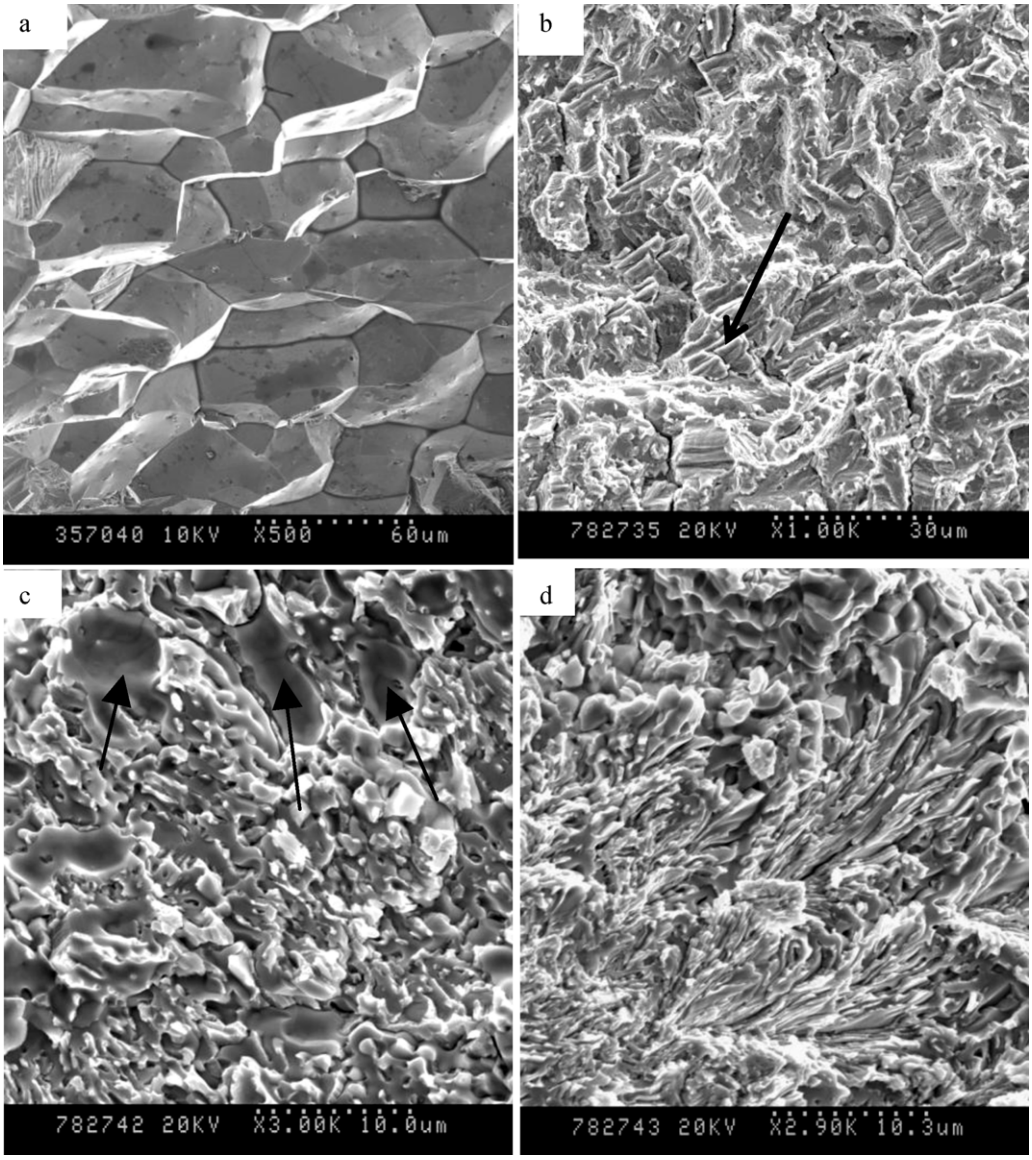

Fig. 5. SEM fractographs of $Ni_{50}Mn_{29}Ga_{21-x}Dy_x$ alloys.(a) $x = 0$; (b) $x = 1$; (c) $x = 5$ and (d) $x = 5$.

effectively hinders the movement of dislocations and the propagation of the cracks, which is one reason for the enhancement of the compressive strength and compressive strain. However, for the $Ni_{50}Mn_{29}Ga_{19}Dy_2$ alloy, although the grains are more refined, the benefits resulting from the refinement effect are offset by the thick network distribution and local enrichment of the $Dy(Ni,Mn)_4Ga$ phase, which results in the decrease of the compressive strain and gradual increase in compressive strength. In the case of the $Ni_{50}Mn_{29}Ga_{16}Dy_5$ alloy, a eutectic structure composed of the matrix and $Dy(Ni,Mn)_4Ga$ phase is found. The two phases with lamellar morphology inside the grains have small spacing. The existence of brittle $Dy(Ni,Mn)_4Ga$ phases strongly restrains the deformation of martensite phase, which leads to higher strength.

Fig. 5 shows the fractographs of $Ni_{50}Mn_{29}Ga_{21-x}Dy_x$ ($x = 0$, 1, 5) alloys at room temperature. It can be seen from Fig. 5(a) that the fractograph of the alloy without rare earth addition shows the typical brittle fracture along the grain boundaries. This is the reason for the lower compressive strength. For the $Ni_{50}Mn_{29}Ga_{20}Dy_1$ alloy, some tearing edges are observed, as indicated by the arrow in Fig. 5(b). The fracture surfaces of this alloy exhibit characteristics of ductile transgranular fracture and plastic deformation occurs before fracturing. This fracture form is consistent with the maximum compressive strain of this alloy. Fig. 5(c) and (d) shows fractographs of $Ni_{50}Mn_{29}Ga_{16}Dy_5$ alloy at different area. In local area, the second phases with larger size are torn off from the matrix, as shown with arrows in Fig. 5(c). In another region of the fracture, as shown in Fig. 5(d), radial cracks are observed. By analyzing the fracture morphology of the alloy and taking into account its microstructure, it is recognized that the cracks generate preferentially and propagate rapidly along the phase boundary of Ni–Mn–Ga matrix and $Dy(Ni,Mn)_4Ga$ phase. This means that for the $Ni_{50}Mn_{29}Ga_{16}Dy_5$ alloy with excessive Dy addition, interphase fracture is observed, which leads to the increase in the brittleness.

3.3. *Magnetic properties of $Ni_{50}Mn_{29}Ga_{21-x}Dy_x$ alloys*

Fig. 6 shows the temperature dependence of AC susceptibility for $Ni_{50}Mn_{29}Ga_{21-x}Dy_x$ ($x = 0$, 0.1, 0.5, 1, 2) alloys during cooling and heating process. The magnetic transition of $Ni_{50}Mn_{29}Ga_{16}Dy_5$

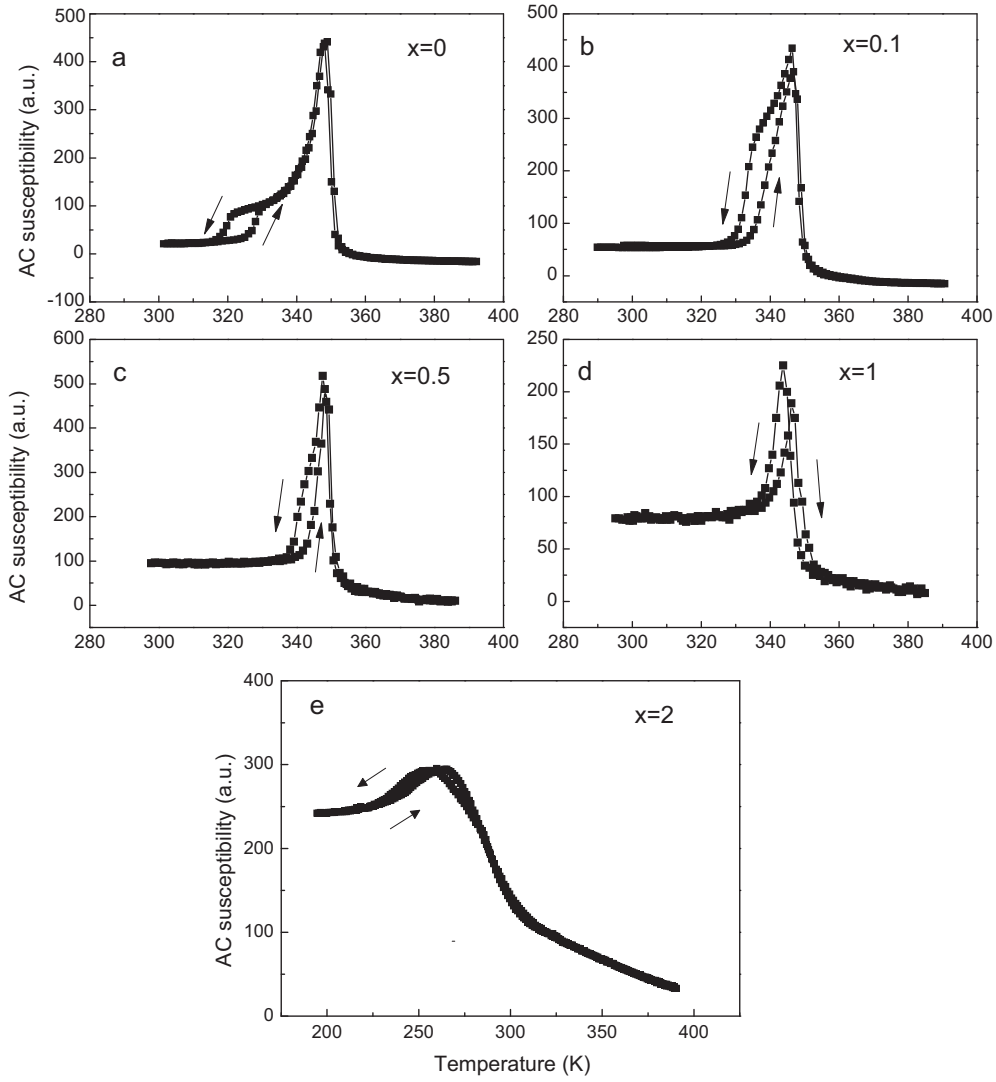

Fig. 6. Temperature dependence of AC susceptibility for $Ni_{50}Mn_{29}Ga_{21-x}Dy_x$ alloys during the cooling and heating process.

alloy could not be detected within the testing range, and the result is not included in the figure. It can be seen that the AC susceptibility curve of $Ni_{50}Mn_{29}Ga_{20.9}Dy_{0.1}$ alloy is similar to that of $Ni_{50}Mn_{29}Ga_{21}$ alloy. During cooling from the high temperature parent phase, two anomalies of the AC susceptibility curve are observed for the two alloys, representing the magnetic and structural transitions, respectively. It is also found that the addition of 0.1 at.% Dy has a small effect on the Curie temperature, while the martensite transformation temperatures increase slightly. When $x = 0.5$, a sharp peak appears in the curves of AC susceptibility during the heating and cooling process, showing that the magnetic transition temperature is near the reverse martensitic transformation finish temperature. This implies a further increase in martensitic transformation temperature and a small change of Curie temperature. As shown in Fig. 6(c), as the content of Dy is 1 at.%, the AC susceptibility enhances sharply and then decreases quickly during the heating process, indicating that the martensitic and magnetic transitions occur simultaneously. Many ternary Ni–Mn–Ga alloys have been found to exhibit this coupling of structural and magnetic transitions [18,19]. Moreover, the largest magnetic entropy change (86 J/kg K) was observed in $Ni_{55}Mn_{20}Ga_{25}$ single crystal under a magnetic field of 5 T [19], and this utilizes the concurrence of structural and magnetic transitions. Thus, the coincidence of martensitic and magnetic transitions in $Ni_{50}Mn_{29}Ga_{20}Dy_1$ alloy can be expected to cause a large magnetic entropy change, which is the subject of an on-going investigation in our group. As for the $Ni_{50}Mn_{29}Ga_{19}Dy_2$ alloy, there is only one abrupt change in the AC susceptibility curve, being relatively slower than other alloys. This indicates that the $Ni_{50}Mn_{29}Ga_{19}Dy_2$ alloy may have weaker magnetic property. According to the DSC results, the martensitic transformation start temperature of this alloy is 399 K. Therefore, the abrupt change of AC susceptibility corresponds to the Curie temperature. It is obvious that the addition of 2 at.% Dy decreases T_c from 351 to 300 K. The experimental results show that the Dy addition causes the formation of $Dy(Ni, Mn)_4Ga$ phases, which contain lower Mn compared with the nominal composition of $Ni_{50}Mn_{29}Ga_{21-x}Dy_x$ alloys. The formation of $Dy(Ni,Mn)_4Ga$ phases results in a significant Mn enrichment in the matrix. Furthermore, the volume fraction of this phase increases gradually as the content of Dy increases to 2 at.%. This leads to a continual increase in Mn content in the matrix. The EDS results reveal that the content of Mn in the matrix increases from 27.99 at.% for ternary $Ni_{50}Mn_{29}Ga_{21}$ alloy to 31.74 at.% for the 2 at.% Dy-doped alloy. Meanwhile, the Ni content in the matrix almost remains unchanged, at nearly 50 at.%, and a decrease in Ga content occurs by the substitution of Dy. The partial Mn atoms exhibit antiferromagnetical coupling with the neighboring Mn atoms. Therefore, the Mn–Mn exchange interaction is weakened, which may result in a decrease of the Curie

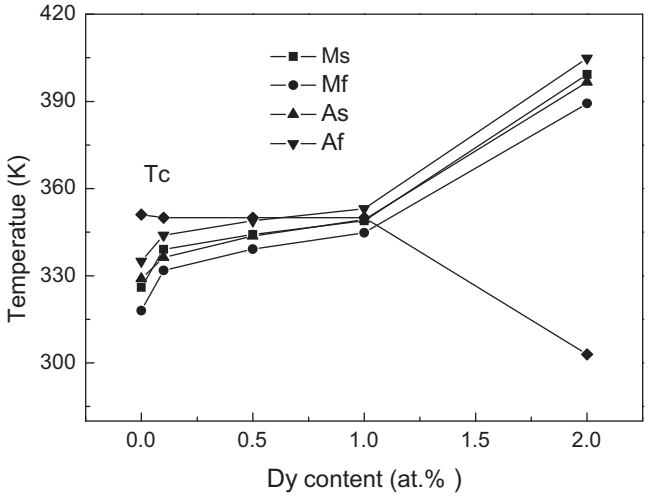

Fig. 7. The transformation temperatures, M_s, M_f, A_s and A_f, and the Curie temperature, T_c, vs. Dy content in $Ni_{50}Mn_{29}Ga_{21-x}Dy_x$ ($x = 0, 0.1, 0.5, 1, 2$) alloys.

temperature. However, the exact mechanism on the change of T_c by adding Dy is not clearly understood, further investigation is needed.

Based on the results of DSC and AC susceptibility measurements, M_s, M_f, A_s, A_f and T_c as a function of the Dy content are presented in Fig. 7. As the content of Dy is no more than 1 at.%, T_c remains almost unchanged, while the martensitic transformation temperature increases gradually with the increase in Dy content. This leads to the magnetic transition temperature being near or equal to the martensitic transformation temperature. When the content of Dy is increased to 2 at.%, a rapid increase in the martensitic transformation temperature is observed, but the excessive addition of Dy weakens the magnetic property and leads to an obvious decrease in the Curie temperature.

4. Conclusions

The effects of Dy addition on the mechanical and magnetic properties of Mn-rich $Ni_{50}Mn_{29}Ga_{21-x}Dy_x$ ($0 \le x \le 5$) ferromagnetic shape memory alloy were investigated. The results show that an appropriate amount of Dy addition in $Ni_{50}Mn_{29}Ga_{21-x}Dy_x$ alloys significantly enhances the compressive strength and improves the ductility. When the content of Dy is less than or equal to 1 at.%, both the compressive strength and strain enhances dramatically, and the compressive strain reaches its maximum value at 1 at.% Dy. The compressive strength remains stable, while the compressive strain decreases remarkably with a further increase in Dy content. Furthermore, the fracture type of Ni–Mn–Ga–Dy alloys changes from intergranular fracture of Ni–Mn–Ga alloys to transgranular cleavage fracture with increasing Dy content. For the alloy with 5 at.% Dy addition, interphase fracture is observed, which leads to an increase in the brittleness. At the same time, a minor Dy addition, i.e. no more than 1 at.%, has little influence on the Curie temperature. However, when the content of Dy is increased to 2 at.%, the Curie temperature decreases. In particular, coupling of the magnetic and structural transitions is observed in the $Ni_{50}Mn_{29}Ga_{20}Dy_1$ alloy. Consequently, the Dy content has a significant influence on the mechanical and magnetic properties. By controlling the amount of rare earth Dy ($0.1 \le x \le 1$) in $Ni_{50}Mn_{29}Ga_{21-x}Dy_x$ alloys, a significant improvement in the compressive strength and ductility of the alloys, an unchanged Curie temperature and increased martensitic transformation temperatures can be achieved.

References

[1] V.A. Chernenko, E. Cesari, V.V. Kokorin, I.N. Vitenko, Scr. Metall. Mater. 33 (1995) 1239–1244.
[2] K. Ullakko, J.K. Huang, C. Kantner, R.C. O'Handley, V.V. Kokorin, Appl. Phys. Lett. 69 (1996) 1966–1968.
[3] G.H. Wu, C.H. Yu, L.Q. Meng, J.L. Chen, F.M. Yang, S.R. Qi, W.S. Zhan, Z. Wang, Y.F. Zheng, L.C. Zhao, Appl. Phys. Lett. 75 (1999) 2990–2992.
[4] J. Pons, V.A. Chernenko, R. Santamarta, E. Cesari, Acta Mater. 48 (2000) 3027–3028.
[5] S.J. Murray, M. Marioni, P.G. Tello, S.M. Allen, R.C. O'Handley, J. Magn. Magn. Mater. 226–230 (2001) 945–947.
[6] A. Sozinov, A.A. Likhachev, N. Lanska, K. Ullakko, Appl. Phys. Lett. 80 (2002) 1746–1748.
[7] W. Cai, L. Gao, A.L. Liu, J.H. Sui, Z.Y. Gao, Scr. Mater. 57 (2007) 659–662.
[8] R.K. Singh, M.M. Raja, R.P. Mathur, M. Shamsuddin, J. Alloys Compd. 506 (2010) 73–76.
[9] X. Zhang, J.H. Sui, Z.L. Yu, W. Cai, J. Alloys Compd. 31 (2011) 8032–8037.
[10] K. Tsuchiya, A. Tsutsumi, H. Ohtsuka, M. Umemoto, Mater. Sci. Eng. A 378 (2004) 370–376.
[11] L. Gao, W. Cai, A.L. Liu, L.C. Zhao, J. Alloys Compd. 425 (2006) 314–317.
[12] S.H. Guo, Y.H. Zhang, Z.Q. Zhao, Y. Qi, B.Y. Quan, X.L. Wang, J. Rare Earths 22 (2004) 875–877.
[13] Z.Q. Zhao, W. Xiong, S.X. Wu, X.L. Wang, J. Iron Steel Res. 111 (2004) 55–58.
[14] L. Gao, Z.Y. Gao, W. Cai, L.C. Zhao, Mater. Sci. Eng. A 438–440 (2006) 1077–1080.
[15] L. Gao, J.H. Sui, W. Cai, J. Magn. Magn. Mater. 320 (2008) 63–67.
[16] J.H. Sui, X. Zhang, L. Gao, W. Cai, J. Alloys Compd. 509 (2011) 8692–8699.
[17] L. Gao, J.H. Sui, W. Cai, Z.Y. Gao, Solid State Commun. 149 (2009) 257–260.
[18] A.A. Cherechukin, T. Takagi, M. Matsumoto, V.D. Buchel'nikov, Phys. Lett. A 326 (2004) 146–151.
[19] M. Pasquale, C.P. Sasso, L.H. Lewis, L. Giudici, T. Lograsso, D. Schlage, Phys. Rev. B 72 (2005) 094435–094439.